Hindawi
Advances in Meteorology
Volume 2018, Article ID 8202031, 11 pages
https://doi.org/10.1155/2018/8202031

Research Article

A Dynamical *Z-R* Relationship for Precipitation Estimation Based on Radar Echo-Top Height Classification

Wenxin Wu,[1,2] **Haibo Zou**,[1] **Jiusheng Shan**,[1] **and Shanshan Wu**[3]

[1]*Meteorological Disaster Emergency Warning Centre of Jiangxi, Nanchang 330096, China*
[2]*Shangrao Meteorological Bureaus, Shangrao 334000, China*
[3]*Jiangxi Climate Centre, Nanchang 330096, China*

Correspondence should be addressed to Haibo Zou; zouhaibobo@sohu.com

Received 7 April 2018; Revised 25 June 2018; Accepted 12 July 2018; Published 19 August 2018

Academic Editor: Hisayuki Kubota

Using echo-top height and hourly rainfall datasets, a new reflectivity-rainfall (*Z-R*) relationship is established in the present study for the radar-based quantitative precipitation estimation (RQPE), taking into account both the temporal evolution (dynamical) and the types of echoes (i.e., based on echo-top height classification). The new *Z-R* relationship is then applied to derive the RQPE over the middle and lower reaches of Yangtze River for two short-time intense rainfall cases in summer (2200 UTC 1 June 2016 and 2200 UTC 18 June 2016) and one stratiform rainfall case in winter (0000 UTC 15 December 2017), and then the comparative analyses between the RQPE and the RQPEs derived by the other two methods (the fixed *Z-R* relationship and the dynamical *Z-R* relationship based on radar reflectivity classification) are accomplished. The results show that the RQPE from the new *Z-R* relationship is much closer to the observation than those from the other two methods because the new method simultaneously considers the echo intensity (reflecting the size and concentration of hydrometers to a certain extent) and the echo-top height (reflecting the updraft to a certain extent). Two statistics of 720 rainfall events in summer (April to June 2017) and 50 rainfall events in winter (December 2017) over the same region show that the correlation coefficient (root-mean-squared error and relative error) between RQPE derived by the new *Z-R* relationship and observation is significantly increased (decreased) compared to the other two *Z-R* relationships. Besides, the new *Z-R* relationship is also good at estimating rainfall with different intensities as compared to the other two methods, especially for the intense rainfall.

1. Introduction

Radar quantitative precipitation estimation (RQPE) has finer temporal and spatial resolutions than those of traditional gauge-based station rainfall observations and can accurately reflect the nonuniformness of the precipitation over a large area [1–3]. Therefore, RQPE is of great importance to severe weather monitoring, industrial and agricultural production, natural disasters prediction and preventing, and even weather modification [4–6]. In practice, the value of RQPE is computed through a nonlinear empirical relationship between radar reflectivity (Z) and precipitation rate (R), $Z = aR^b$, where a and b are two parameters to be determined [7–9].

In early studies, a simple *Z-R* relationship can be obtained statistically over a climatic timescale and then applied to the quantitative estimate of precipitation. Different regions usually yield quite different parameters [10, 11]. The RQPE obtained from the U.S. WSR-88D radar system obeys the relationship of $Z = 300R^{1.4}$ in extratropical regions, while obeys $Z = 250R^{1.2}$ in the tropical regions [12]. In China mainland, the RQPE obtained from China New Generation Weather Radar (CINRAD) system follows the fixed relationship of $Z = 300R^{1.4}$. In fact, there is considerable variation in the coefficients a and b, and they are significantly affected by the characteristics of raindrop-sized spectra [7, 13]. Therefore, the parameters a and b in the *Z-R* relationship are affected by synoptic weather situations, hydrology, geography, and so on and thus vary with time and space. Such a fact could produce different values of these parameters in different climates and even different rainfall events [14–17]. Rosenfeld and Ulbrich [18] also discuss the

differences in the Z-R relationship between maritime and continental, convective, transition and stratiform, and orographic precipitation. Therefore, a fixed Z-R relationship may not be accurate for a rainfall event with different intensities.

From then on, in order to obtain a more complex and accurate Z-R relationship, precipitation is categorized into different types (or radar reflectivity is classified into different intensities). Then, a set of Z-R relationships in different types of precipitation are derived. This method is well known as the classification Z-R relationship and has been a great improvement in accuracy [19, 20]. Besides, Alfieri et al. [21] assumed that the Z-R relationship changes with time and pointed out that the Z-R relationship within a specific time should be determined by the reflectivity and rainfall during that time (i.e., dynamical Z-R relationship). The method of the dynamical Z-R relationship also improves the accuracy of RQPE.

Although the above two methods (classification Z-R relationship and dynamical Z-R relationship) improve the accuracy of RQPE, they both have obvious shortcomings. The classification Z-R relationship (i.e., the method in [19] and [20]) does not take into account the possible temporal variation of the relationship, while the dynamical Z-R relationship (i.e., the method in [21]) does not take into account different types of precipitation. With the advantages of the classification Z-R relationship and dynamical Z-R relationship, Wang et al. [22] proposed a dynamical Z-R relationship based on radar reflectivity classification. a and b in this Z-R relationship vary with the time and echo strength. This method is shown to have both advantages of the previous two methods and thus further improves the accuracy of RQPE [22].

Previous works mainly focused on the spatial or temporal variation of the empirical coefficients a and b in the Z-R relationship, while Wang et al. [22] simultaneously consider their spatial and temporal variation. They categorize observational precipitation and reflectivity into different groups based on the radar reflectivity and then dynamically (in different times) calculate the coefficients a and b in the Z-R relationship in different groups. Although the radar reflectivity value (echo strength) is closely related to the size and concentration of hydrometeors in a sampled area [18] and can directly reflect the rain rate of a storm to a certain extent, the echo-top (ET) height is also a good indicator of rain rate. Adler and Mack [23] and Atlas et al. [24] noted that the rain rate in a storm is determined by the updraft and the vertical gradient of saturation vapor density (which can change the content of hydrometeors), and the storm height (i.e., the echo-top height) is also determined essentially by the updraft velocity. Adler and Mack [23] and Rosenfeld et al. [25] have shown that the echo-top (ET) height is well correlated with rain rate. Bedka et al. [26] also implied that the ET height is more representative to the development of a storm and rainfall system. Also, ET height can be used to identify the ground clutters based on the different features between meteorological echoes and ground clutters [27]. Owing to the advantages of ET height, Rosenfeld et al. [25] utilized it to develop the height-area rainfall threshold (HART) method to estimate the mean convective rainfall over an area (i.e., an averaged value over an area) and show better results. Therefore, using ET height instead of radar reflectivity to categorize observational precipitation and reflectivity into different groups is expected to further improve the accuracy of RQPE because the new method simultaneously considers the content of hydrometers (radar reflectivity) and the updraft (ET height) of a storm to a certain extent. Section 2 introduces the study area and data processing procedure. Section 3 describes the dynamical Z-R relationship based on reflectivity classification, and Section 4 depicts the new constructed Z-R relationship based on ET height classification. Section 5 shows the performance of the new Z-R relationship to derive RQPE. Conclusions are given in the final section.

2. Data Source and Processing

The area of interest in the present study is over the middle and lower reaches of Yangtze River (113–119°E, 27.5–31°N), where short-time intense precipitation (rain intensity more than $10\,\mathrm{mm{\cdot}h^{-1}}$) occurs very frequently in the summer time (April–August). This area includes six provinces of Jiangxi, Anhui, Zhejiang, Hunan, Hubei, and Fujian in China, containing 3468 automatic rainfall observational stations and 12 CINRAD Doppler radars (Figure 1). The observed radar and rain gauge data are provided by the Meteorological Information Center of the Jiangxi (in China) Meteorological Administration (JMA) and can be accessed from the CMISS interface (http://10.116.89.55/cimissapiweb/) at the Intranet of JMA.

When estimating the rainfall using the reflectivity of the Doppler radar, it is common to use the echoes on the constant-altitude plan position indicator [28] at 1.5 km from the sea level or echoes at low elevation angles [29]. However, in the area of interest here, there are some blind regions in the radar CAPPI at 2 km due to the uneven distribution and different altitudes of radar stations. Besides, there are also mountains (elevation larger than 600 m) within 30 km for several radar stations (Shangrao, Yichun, and Quzhou) that prevent the detection of radar beams at small elevation angles (i.e., some radar beams at small elevation angles may be blocked by surrounding mountains). Therefore, in this area, the radar mosaic of composite reflectivity (CR) is used for RQPE instead of using 1.5 km CAPPI and small-angle echoes. CR is accomplished through four steps. Firstly, radar reflectivity data in polar coordinates are processed to remove isolated nonmeteorological echoes and ground clutters using the improved quality control method in [30]. Then, the horizontal interpolation with the nearest neighbor on the range-azimuth plane [31] is selected to convert radar data in polar coordinates into a regular latitude/longitude grid of 0.01° resolution. Thirdly, the maximum value of CR in different radars is used as the value of the radar mosaic for overlapping regions. Finally, a 9-point smooth operator is applied to yield the final mosaic for each time. The processes of the mosaic in ET height are similar to those in CR. Here, the ET height is calculated using the improved method of [32]. The algorithm is as follows.

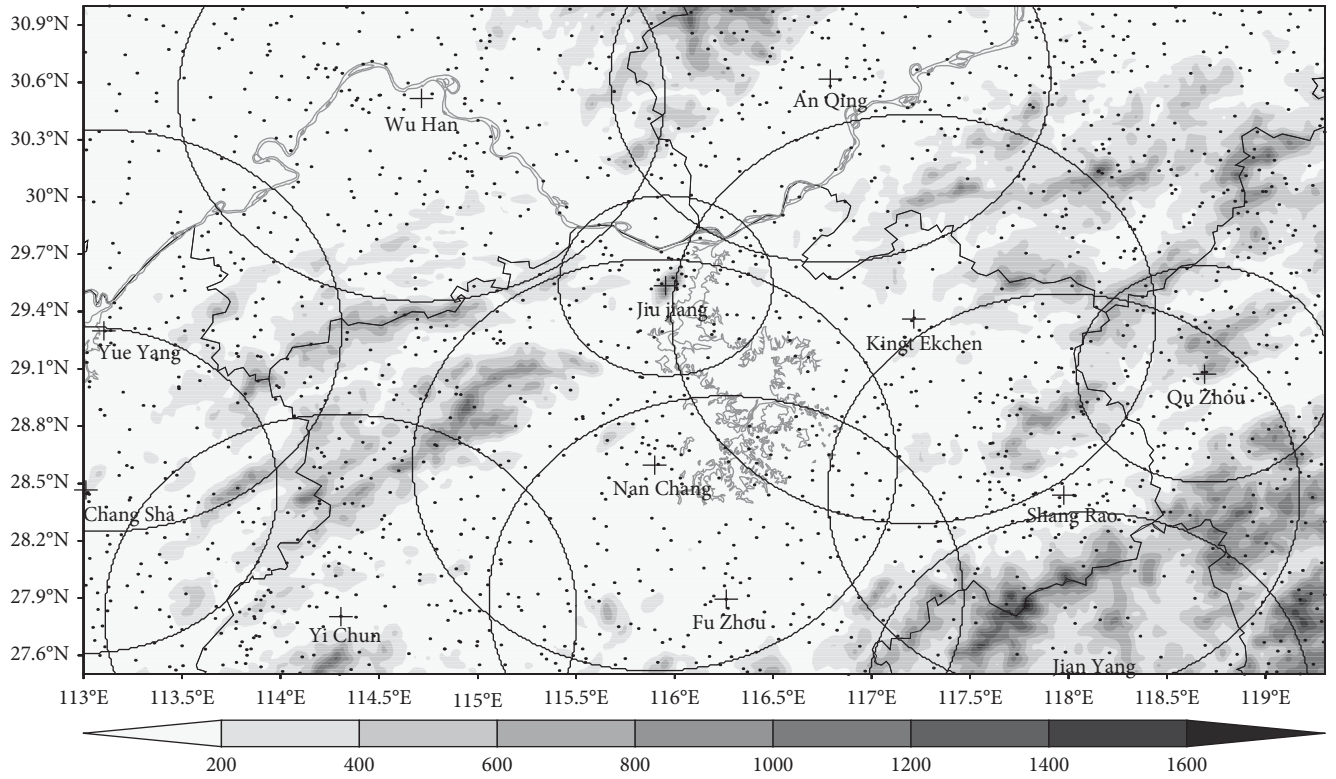

Figure 1: Doppler radar stations (cross point) and automatic rainfall observation stations (dot) over the middle and lower reaches of Yangtze River. Circles indicate the range of CAPPI at 2 km height and shaded portions indicate altitude (unit: m).

$$\theta_{\mathrm{T}} = \left(Z_{\mathrm{T}} - Z_a\right)\frac{\left(\theta_b - \theta_a\right)}{\left(Z_b - Z_a\right)} + \theta_b, \tag{1}$$

where θ_b is the maximum elevation angle where the reflectivity value Z_b exceeds the echo-top reflectivity threshold Z_{T} (e.g., 18 dBZ). θ_a and Z_a are the elevation angle and reflectivity value at the next higher elevation angle of θ_b. θ_{T} obtained by (1) is an elevation angle rather than a height over the radar site. The radar beam height (i.e., the ET height) of θ_{T} can be calculated by the method of [33]:

$$\left(R^2 + R_W^2 + 2R \cdot R_W \cdot \sin\theta\right)^{1/2} - R_W = 4.5. \tag{2}$$

The improved method for obtaining ET height (e.g., (1)) is proposed that echo tops be computed by interpolating between elevation scans that bracket the echo-top threshold and results in smaller errors when higher-elevation scans are available [32].

3. Dynamical *Z-R* Relationship Based on Echo Intensity Classification

The parameters a and b in the Z-R relationship are affected by local weather, hydrology, geography, and so on. Therefore, different regions in a given time or different times in a given region usually correspond to different parameters a and b. In other words, the parameters a and b vary with time and space. Liu et al. [20] and Chumchean et al. [19] take into account the spatial variation (i.e., classification of precipitation) and Alfieri et al. [21] consider the temporal variation (i.e., dynamical fitting of a and b using observational rainfall and reflectivity in a given time) to construct the Z-R relationship. Wang et al. [22] proposed a Z-R relationship which has simultaneously taken into account the spatial variation (classification based on radar reflectivity) and temporal variation (dynamical fitting) of a and b (e.g., dynamical Z-R relationship based on echo intensity classification). This method significantly improves the accuracy of RQPE compared to that of [19] and [21].

The dynamical Z-R relationship based on echo intensity classification is designed as follows [22]: Firstly, getting the CR mosaic using the maximum-value-based composite method introduced in Section 2. Secondly, averaging the CR mosaic over a specific time (one hour in the present study), as well as obtaining the accumulated amount of observational precipitation in different sites over the same time. Thirdly, classifying the averaged CR into different groups according to the interval of 5 dBZ (i.e., 5, 10, 15, 20, 25, 30, 35, 40, 45, 50, 55, 60, 65, 70, and 75 dBZ). Fourthly, the accumulated precipitations are also classified into different groups according to the groups of CR. Fifthly, the Z-R relationships in different groups (e.g., the CR group of 30 dBZ and the corresponding precipitation group) are determined by fitting the CR to the precipitation using the optimizing method developed in [34]. A set of a and b corresponding to different groups are obtained in the given time, yielding a "best-fit" Z-R relationship for the time. The optimizing

method proposed in [34] is to obtain the minimum values of a criterion function (CTF) which is expressed as follows:

$$\mathrm{CTF} = \min\left\{\sum_{i=1}^{n}\left[\left(H_{i,j,k} - G_i\right)^2 + \left(H_{i,j,k} - G_i\right)\right]\right\}, \quad (3)$$

where G_i is the observed precipitation at station i and n is the number of stations. The estimated precipitation $H_{i,j,k}$ is calculated by the Z-R relationship at station i as

$$H_{i,j,k} = 10^{\left(\log Z_i - \log a_j\right)/\left(b_k/100\right)}, \quad (4)$$

where $a_j = 1, 2, \ldots, 1200$, $b_k = 100, 101, \ldots, 300$, and Z_i is the reflectivity value at station i. The best value of a and b (i.e., the most suitable Z-R relationship) is obtained through iteratively computing CTF to get the minimum value. Ciach et al. [35] and Chumchean et al. [19] used a very similar method to get the Z-R relationships. Finally, repeatedly performing the above 1–5 steps in different times (i.e., dynamical) can induce the coefficients a and b in the Z-R relationship to vary with the reflectivity intensity and time, finally forming the dynamical Z-R relationship based on echo intensity classification.

4. Dynamical Z-R Relationship Based on ET Classification

Radar ET height is defined as the radar beam height at the highest elevation angle where the detected reflectivity value is not less than a threshold of 18 dBZ. ET height not only can reflect the storm development stage and precipitation system intensity [26] but also can identify ground clutters since they have a relatively low ET height [27]. Therefore, it has been widely used in weather forecasting and synoptic diagnostics [36, 37] (Evens, 2004). Table 1 shows the mean correlation coefficients between echo intensity or ET height and observational rainfall in the region of Figure 1 during April and May 2017. It is clear that the correlation coefficients between both of them are greater than 0.5, and the correlation coefficient between observational precipitation and ET height is slightly large in both April and May 2017. This further confirms that ET height can be an indicator of rainfall intensity very well. Besides, although two storms with the same reflectivity and different ET heights in the conical surface may have a similar amount of hydrometeors (Figure 2), they may yield different precipitation rates because the rain rate is well related to the updraft and the ET height is the embodiment of the updraft (Adler and Mack, 1984) [24]. Therefore, if the two storms are grouped by ET height, they may have different precipitation rainfall because they are classified into different groups. But if they are grouped by echo intensity, they belong to a same group and yield the same precipitation. Therefore, the Z-R relationship based on ET height classification (rather than reflectivity classification) may further improve the accuracy of RQPE.

The procedure of the dynamical Z-R relationship based on ET height classification is similar to that of the dynamical Z-R relationship based on echo intensity which has been depicted in Section 3, except for echo classification using ET height instead of reflectivity intensity. The specific steps are as follows: firstly, getting the CR mosaic and ET height mosaic using the maximum-value-based method introduced in Section 2. Secondly, averaging the CR mosaic and ET height mosaic over a specific time (one hour in the present study), as well as obtaining the accumulated amount of observational precipitation over the same time. Thirdly, the averaged CR is classified into different groups based on the ET height with 1 km interval (i.e., 1, 2, 3, 4, 5, 6, 7, 8, 9, 10, 11, 12, 13, 14, and 15 km). The 4–6 steps are the same as those of the dynamical Z-R relationship based on echo intensity which has been depicted in Section 3.

Table 1: The correlation coefficients between reflectivity/ET height and observational rainfall.

Time	Composite reflectivity	ET height
April 2017	0.508	0.522
May 2017	0.505	0.510

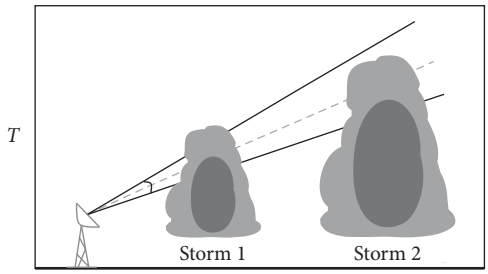

Figure 2: Schematic illustrations of two storms with the same echo intensity and different ET heights.

5. Results

The study [26] and the correlation analysis in Section 4 have shown that ET height can reflect preferably the development of storm. Therefore, the dynamical Z-R relationship based on ET height classification is expected further to improve the accuracy of RQPE. To verify this, three methods (Z-R relationships) are used to derive RQPE and then compared to observational precipitation. The three methods are the fixed-parameter algorithm (SM), dynamical Z-R relationship based on echo intensity classification (EIDM) developed in [22], and dynamical Z-R relationship based on ET height classification (ETDM) developed in this paper.

5.1. Case Study. We choose two short-time intense rainfall events (occurred, resp., at 2200 UTC 1 June 2016 and 2200 UTC 18 June 2016) over the middle and lower reaches of Yangtze River to test the ETDM. For the case happened at 2200 UTC 18 June 2016, precipitation was mainly located at the northern part of Jiangxi Province and the border regions of provinces of Jiangxi, Hubei, and Anhui, with maximum values exceeding 40 mm·h^{-1} (Figure 3(a)). The main rainfall belt (with precipitation more than 10 mm·h^{-1}) is northwest-southeast distributed. The three methods that derived RQPE

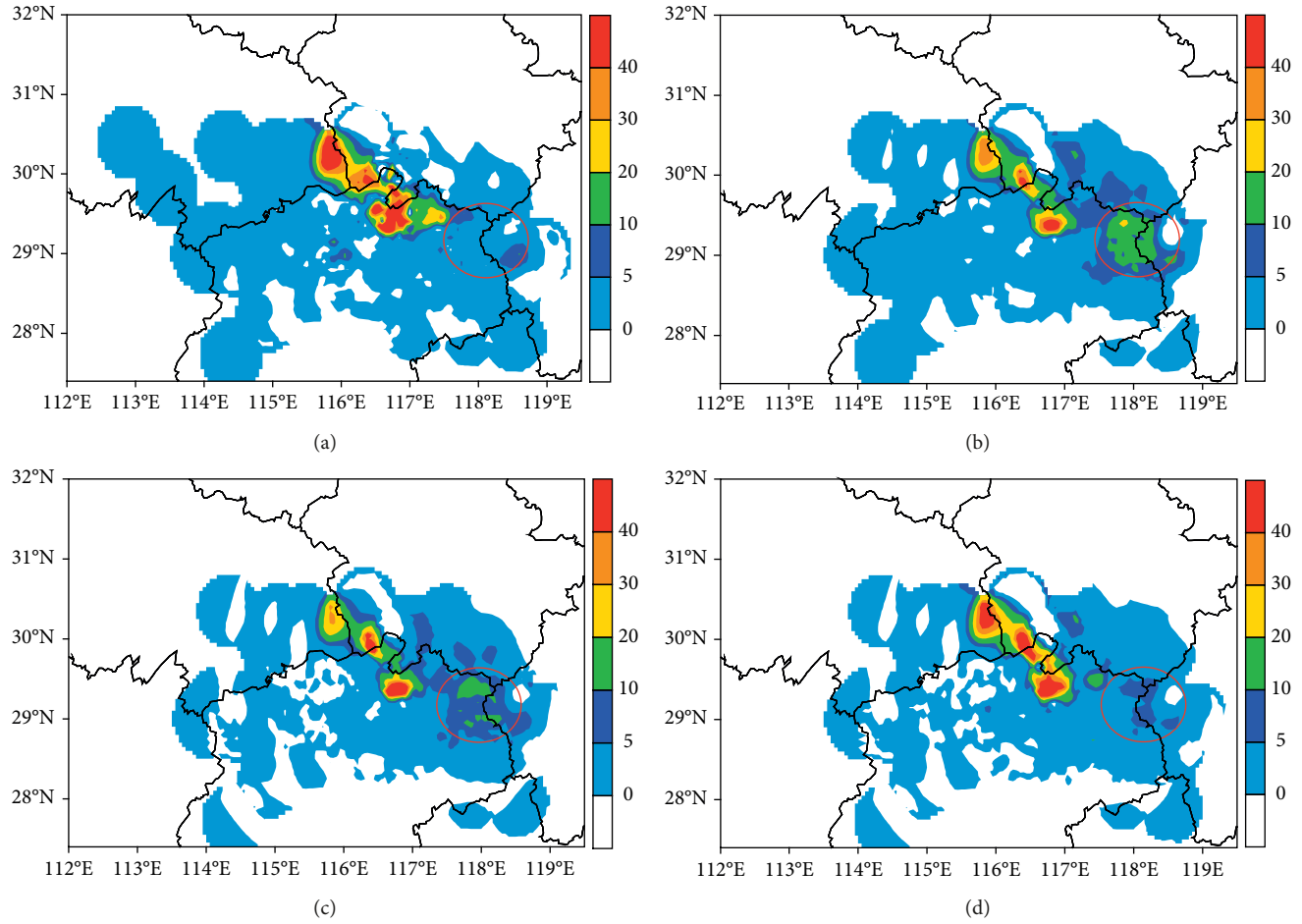

Figure 3: Precipitations (mm) obtained from (a) observation, (b) SM method, (c) EIDM method, and (d) ETDM method at 2200 UTC 18 June 2016.

have been produced with reasonable rainfall distribution (Figure 3(a)). However, it can be seen that the RQPE determined by the SM method (Figure 3(b)) was obviously underestimated, and the area of RQPE exceeding 10 or 30 mm·h^{-1} was significantly decreased. The distribution and value of RQPE derived by EIDM (Figure 3(c)) are very similar to those of SM (Figure 3(b)), except for that the SM overestimates the RQPE in the red circle region in Figure 3. By comparison, the ETDM obtains the best RQPE (Figure 3(d)) in both magnitude and region as compared to the observation (Figure 3(a)). The spatial correlation coefficients between RQPEs estimated by the three methods and observational precipitation (≥0.1 mm·h^{-1}) are 0.76 (SM), 0.80 (EIDM), and 0.88 (ETDM), respectively. This further implies that the ETDM to obtain RQPE is best in the three methods.

In the case of 2200 UTC 1 June 2016, the precipitation was mainly distributed at the northwestern part of Jiangxi Province, with maximum values exceeding 30 mm·h^{-1} (Figure 4(a)). The main rainfall belt (with precipitation more than 10 mm·h^{-1}) is also northwest-southeast orientated. Like the case of 2200 UTC 18 June 2016, all three methods (SM, EIDM, and ETDM) have successfully derived the distribution of precipitation (Figures 4(b)–4(d)). But the RQPE determined (Figure 4(b)) by the SM method is consistently smaller than observations over the areas with rainfall exceeding 15 mm·h^{-1}, as shown in Figure 4(a). By comparison, the EIDM improves the accuracy of RQPE, with an obvious increase in precipitation (with the maximum rainfall exceeding 30 mm·h^{-1}). But the rainfall intensity is still smaller than that of observation. More importantly, the ETDM (Figure 4(d)) conspicuous improved RQPE quality which is more close to the observation (Figure 4(a)). The spatial correlation coefficients between RQPEs determined by the three methods and observational precipitation (more than 0.1 mm·h^{-1}) are 0.68 (SM), 0.72 (EIDM), and 0.74 (ETDM), respectively. The ETDM has still the largest correlation coefficient in the three methods.

The above two short-time intense rainfall cases (2200 UTC 1 June 2016 and 2200 UTC 18 June 2016) have shown the well performance of ETDM to derive RQPE. Why ETDM has better performance than EIDM? In fact, the EIDM (ETDM) is constructed by classifying CR and precipitation into different groups based on echo intensity (ET height), and the parameters a and b in the Z-R relationship are fitted by the CR values and the observed precipitations for a specific group. If there are more samples with intense (weak) precipitation in the group, the fitted Z-R relationships will derive intense (weak) RQPE. The distributions of CR, ET height, and

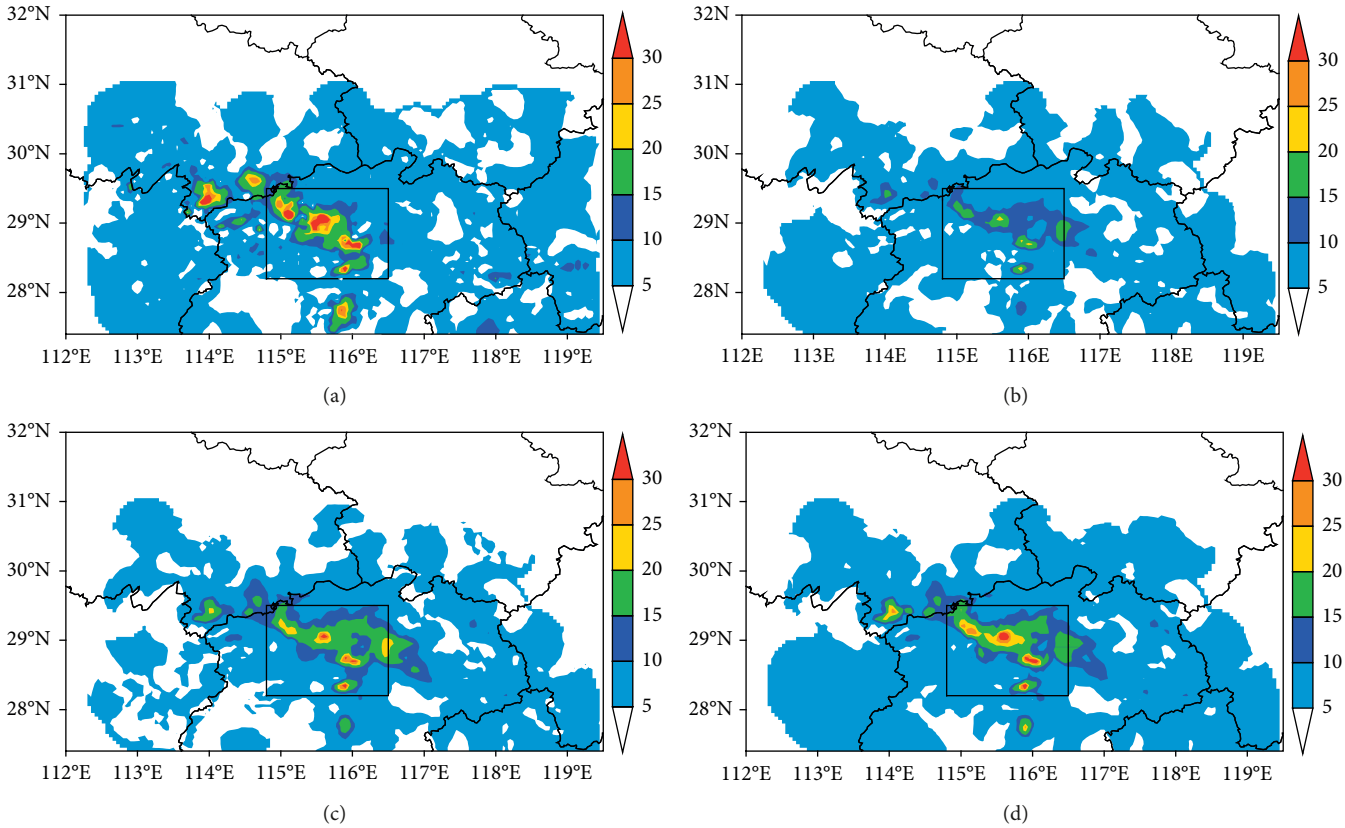

Figure 4: Precipitations (mm) obtained from (a) observation, (b) SM method, (c) EIDM method, and (d) ETDM method at 2200 UTC 1 June 2016.

precipitation in the rectangular region in Figure 4 are shown in Figure 5. As shown in Figure 5, the strong precipitation occurs in the areas of strong radar echo (≥35 dBZ) and high ET height (≥9 km). But the high ET height corresponds better to the intense precipitation than the large CR. For example, a region with relatively weak precipitation (6 mm·h^{-1}), strong echoes (exceeding 40 dBZ), and relatively low ET height (less than 9 km) appears at the black circle area in Figure 5. This indicates that when constructing the *Z-R* relationships using EIDM, the group (especially for the group that included most intense precipitation samples) may contain more weak precipitation samples than using the ETDM. The more weak precipitation samples will result in that the EIDM underestimates the RQPE than the ETDM (e.g., Figures 3(c), 3(d), 4(c), and 4(d)).

Although the new method based on ET classification to derive RQPE performs better than the other two methods, the two cases used to test belong to convective storms. Rosenfeld et al. [25] also indicated that a deeper convective storm can more easily produce heavy rain, and a better correlation can be obtained using the classification statistics based on ET height. Therefore, how does the new method performs in nonconvective storm (i.e., stratiform precipitation system)? To answer this question, a stratiform precipitation case that occurred at 0000 UTC 15 December 2017 is selected to further test the new method. At 0000 UTC 15 December 2017, the precipitation mainly fell in the middle and northeastern parts of Jiangxi Province, with maximum values less than 4 mm·h^{-1} (Figure 6(a)). All three methods (SM, EIDM, and ETDM) have successfully derived the precipitation near the maximum precipitation center (i.e., the black square in Figure 6). But precipitations obtained by the three methods are less than the observation. The SM method throws away many areas with precipitation, leading to many scattered precipitation points appeared at the domain (Figure 6(b)). This induces that the correlation coefficient between observation and RQPE derived by SM is only 0.32 which is significantly less than those of the above two convective cases. By comparison, the EIDM estimates more areas with precipitation (Figure 6(c)), increasing the correlation coefficient to 0.55. More importantly, the ETDM not only increases the areas of precipitation but also enlarges the intensity of precipitation (Figure 6(d); the maximum precipitation is more than 2.5 mm·h^{-1}), further increasing the correlation coefficient to 0.58. As shown in Figure 6, all three methods cannot derive the precipitation in the area encircled by the red rectangle which is in fact the mountainous region (Figure 1). This may be induced by the blockage of mountains to the radar beam in lower elevation angles. Zou et al. [30] indicated that this area is also a blind region of the Nanchang radar in 0.5° tilt. It is clear that although the RQPE derived from the stratiform precipitation system is less accurate than that from the convective storm, the ETDM to derive RQPE still has a significant advantage compared with the other methods.

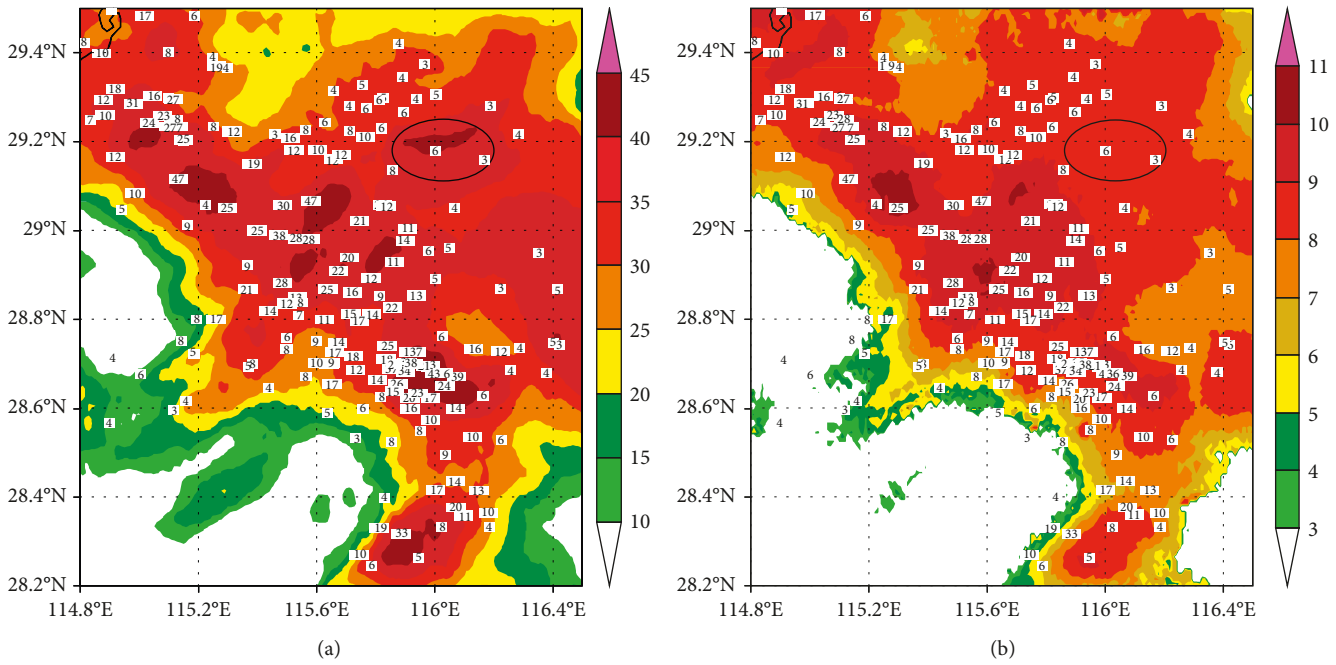

Figure 5: (a) CR (unit: dBZ) and (b) ET (unit: km) in the black rectangle in Figure 4 at 2200 UTC 1 June 2016. Digits show the 1-hour precipitation (mm) observed by rain gauges.

5.2. Statistical Analysis. It has been shown in the above three cases that the ETDM proposed in the present study results in a more accurate RQPE than the traditional SM and EIDM do. Is this viewpoint universality? To address this problem, in the following section, 720 rainfall cases in the summer season (April to June 2017) and 50 rainfall cases in the winter season (December 2017) over the middle and lower reaches of Yangtze River were collected to further compare SM, EIDM, and ETDM methods. The precipitations over the region in the summer time comprise convective rainfall and stratiform precipitation (with a high ET height), while the precipitations occurring in the winter time system are mainly induced by the stratiform system (with a lower ET height). Three statistics, correlation coefficient (R), root-mean-squared error (RMSE), and relative error (RE), between RQPEs derived by the three methods and observed precipitation are used to evaluate the performance of each method:

$$R = \frac{\sum_{i=1}^{n}\left(H_i - \overline{H_i}\right)\left(Q_i - \overline{Q_i}\right)}{\sqrt{\sum_{i=1}^{n}\left(H_i - \overline{H_i}\right)^2 \cdot \sum_{i=1}^{n}\left(Q_i - \overline{Q_i}\right)^2}}, \quad (5)$$

$$\mathrm{RMSE} = \sqrt{\frac{1}{n}\sum_{i=1}^{n}\left(H_i - Q_i\right)^2}, \quad (6)$$

$$\mathrm{RE} = \frac{\sum_{i=1}^{n}\left|H_i - Q_i\right|}{\sum_{i=1}^{n} Q_i}. \quad (7)$$

where H_i is the estimated precipitation (according to (4)), Q_i is the observed precipitation at station i, and n is the number of stations with valid rainfall in a given time. The correlation coefficient R reflects the similarity of the spatial patterns between RQPE and observational precipitation, with the bigger the R, the higher the accuracy of RQPE. The RMSE shows the overall deviation of RQPE from the observation, with the smaller the RMSE, the higher the accuracy of RQPE. The RE reflects the overall relative error of RQPE related to observation, with the smaller the RE, the higher the accuracy of RQPE.

Table 2 shows all these statistics in (5)–(7) which are averaged from April to June 2017 (i.e., in the summer season, with a total of 720 rainfall cases) over the middle and lower reaches of Yangtze River. It can be seen from Table 2 that the RQPE derived by the SM is able to preferably reproduce the spatial pattern and amount of observational precipitation, with a correlation coefficient of 0.59, an RMSE of 3.0 mm, and an RE of 69.1%. However, there is a significant improvement for the EIDM to derive RQPE, with a significant increase of correlation coefficient to 0.64, a reduction of RMSE to 2.5 mm, and a decrease of RE to 59%. More importantly, there is also a further improvement for the ETDM to derive RQPE (relative to EIDM), with R increasing to 0.69 (it is 0.1 or 0.05 larger than that of the SM or EIDM, resp.), RMSE reducing to 2.3 mm, and RE decreasing to 56.2%. Therefore, it is shown that there are continuous improvements from SM to EIDM and then to ETDM, which results in more and more accurate RQPE.

To further assess the performances of the three methods to derive RQPE in the winter season (small precipitation and lower ET height), these statistics in (5)–(7) during December 2017 (with a total of 50 rainfall cases) are shown in Table 3. The correlation coefficient between RQPE derived by SM and observation is only 0.44, decreasing by 0.15 compared to that of the summer season (Table 2). Correspondingly,

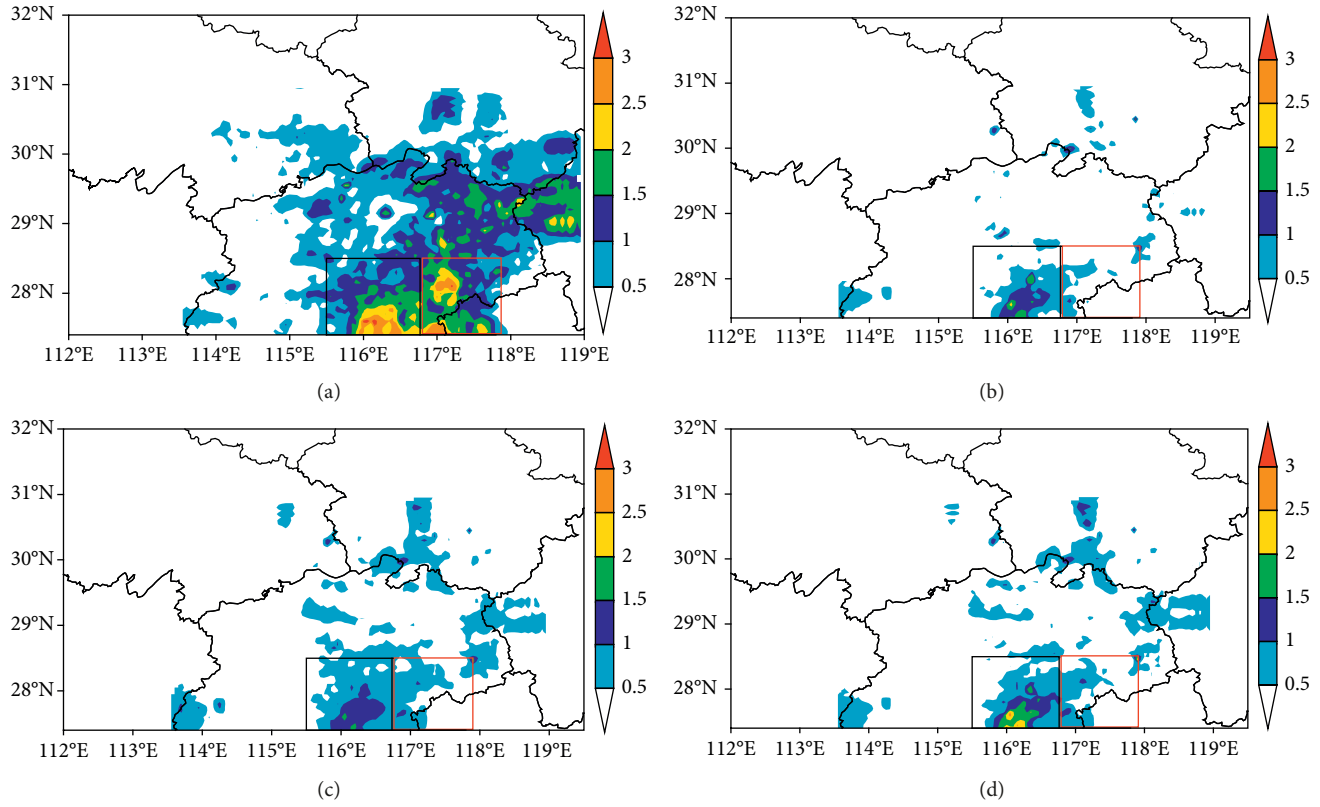

Figure 6: Precipitations (mm) obtained from (a) observation, (b) SM method, (c) EIDM method, and (d) ETDM method at 0000 UTC 15 December 2017.

the relative error RE (70.5%) is more than that of the summer season. Note that the smaller RMSE in the winter season (Table 2) does not reflect the higher accuracy. This is mainly induced by a small amount of precipitation in the winter season. Clearly, the performance of SM in the summer season is better than that in the winter season. Similarly, the EIDM improves the accuracy of RQPE in the winter season on the basis of SM. The correlation coefficient increases to 0.49 accompanied by a reduction of RMSE to 0.63 mm and a decrease of RE to 70.4%. More importantly, the ETDM further improves the accuracy of RQPE on the basis of EIDM so that the correlation coefficient increases to 0.51 followed by a slight decrease in RMSE and RE. It is clear that although the accuracy of RQPE in the winter season is worse than that in the summer season, the ETDM still can improve the accuracy of RQPE derived by EIDM and SM.

The above analysis evaluates the performance of the SM, EIDM, and ETDM to derive RQPE in an overall perspective. It is also interesting to evaluate their performance in deriving RQPE at different rainfall intensities. Here, four intensity levels of 0.1–10 mm, 10–25 mm, 25–50 mm, and above 50 mm are chosen to evaluate the three methods (SM, EIDM, and ETDM). Figure 7 shows the RE (relative error; i.e., (7)) between observed precipitation and the RQPEs obtained by the three methods at different rainfall intensities. It is clear that the RE of the SM (~75%) is close to that of the EIDM when the rainfall amount is less than 10 mm. However, with the increase in rainfall, the RE of both SM and EIDM decreases significantly. When the rainfall amount is larger than or equal to 50 mm, the RE of the SM and EIDM decreases to about 55% and 40%, respectively. It is also shown in Figure 7 that the RE of ETDM is the smallest one at the intensity level of 0.1–10 mm, and then it decreases more rapidly than those of SM and EIDM. Thus, the RE of ETDM is the smallest one at different rainfall intensities, and the RE difference between the ETDM and SM increases with the increase of rainfall intensity. Therefore, it is obvious that the ETDM constructed in the paper is a better choice to derive RQPE at different rainfall intensities, especially for precipitation more than 50 mm which has the smallest RE (~30%). Besides, among the three methods to derive RQPE, the reduction speed of RE of SM is the slowest with the increase of rainfall intensity. This implies that the SM has the worst performance in the three methods to obtain the precipitation rate.

Table 2: Statistics of correlation coefficient (R), root-mean-squared error (RMSE), and relative error (RE) that evaluate the performance of the three methods to derive RQPE during April to June 2017.

Method	R	RMSE (mm)	RE (%)
SM	0.59	3.0	69.1
EIDM	0.64	2.5	59.0
ETDM	0.69	2.3	56.2

Table 3: Statistics of correlation coefficient (R), root-mean-squared error (RMSE), and relative error (RE) that evaluate the performance of the three methods to derive RQPE during December 2017.

Method	R	RMSE (mm)	RE (%)
SM	0.44	0.66	70.5
EIDM	0.49	0.63	70.4
ETDM	0.51	0.62	70.3

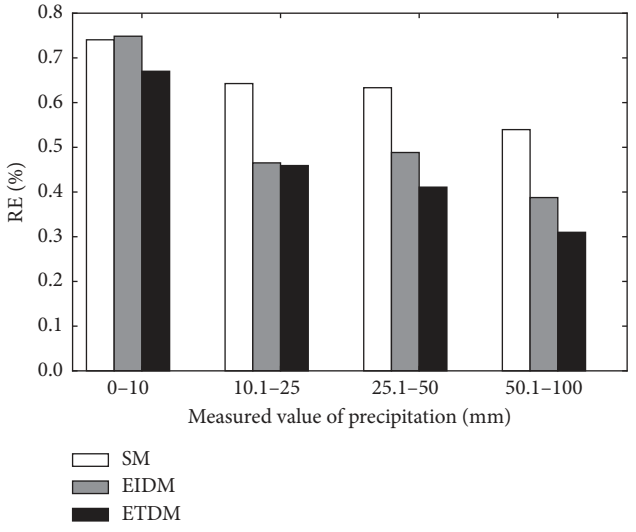

Figure 7: Relative error (%) of RQPE determined from the SM, EIDM, and ETDM methods.

6. Conclusions

In the present study, a new dynamical reflectivity-rainfall (Z-R) relationship is established for the operational RQPE, based on the echo-top (ET) height which can preferably reflect the development of the rainfall storm. Then, it is applied to derive the RQPE over the middle and lower reaches of Yangtze River for three cases (two cases are short-time intense rainfall cases, resp., at 2200 UTC 1 June 2016 and 2200 UTC 18 June 2016, and one is a stratiform rainfall case). The results show that the RQPEs derived from two summer cases are more accurate compared to that from the winter case. More importantly, regardless of the summer case with large precipitation and high ET height or the winter case with small precipitation and low ET height, the new ETDM proposed here is able to derive an RQPE which is much closer to the observation in both magnitude and spatial distribution than the SM and EIDM methods.

To further confirm the performance of the new ETDM, three statistical variables (correlation coefficients, root-mean-squared error, and relative error) between RQPEs derived by the three methods (SM, EIDM, and ETDM) and observed precipitation are used to evaluate their performances to derive RQPE over three summer months (April to June 2017, with a total of 720 rainfall cases) and one winter month (December 2017, with a total of 50 rainfall cases). The results also show that the new ETDM significantly increases the correlation coefficient and reduces the root-mean-squared error and relative error between the RQPE and the observed precipitation regardless of summer or winter. Besides, the new ETDM yields a more accurate RQPE in different intensity rainfalls as compared to the SM and EIDM methods. It is clear that the ETDM-based ET classification further improves the accuracy of derived RQPE compared with the EIDM-based echo intensity classification.

A new dynamical Z-R relationship is established based on ET height classification in this paper. The tests of the three cases (two in summer and one in winter) and two statistics (one in summer and the other one in winter) show that the new Z-R relationship has well performed to derive RQPE. However, the merging results of multiple sources of rainfall rates can provide a better quantity than any single source [38]. Although satellite QPE is limited by a lack of robust correlation between cloud-top brightness temperature and surface rainfall, it is more spatially coherent than radar QPE and is not subject to terrain-based blockages or discontinuities due to lack of data and instrumentation differences [38]. Therefore, future work will focus on the blending of RQPE developed in this paper, satellite rainfall QPE, and rain gauge estimate.

Data Availability

The data used to support the findings of this study are available from the corresponding author upon request.

Conflicts of Interest

The authors declare that they have no conflicts of interest.

Acknowledgments

This study was jointly supported by the Jiangxi Provincial Department of Science and Technology Project (Grant no. 20171BBG70004) and the National Natural Science Foundation of China (Grant no. 41765001).

References

[1] R. A. Scofield and R. J. Kuligowski, "Status and outlook of operational satellite precipitation algorithms for extreme-precipitation events," *Weather and Forecasting*, vol. 18, no. 6, pp. 1037–1051, 2003.

[2] M. Steiner, J. A. Smith, S. J. Burges, C. V. Alonso, and R. W. Darden, "Effect of bias adjustment and rain gauge data quality control on radar rainfall estimation," *Water Resources Research*, vol. 35, no. 8, pp. 2487–2503, 1999.

[3] S.-S. Yoon, A. T. Phuong, and D.-H. Bae, "Quantitative comparison of the spatial distribution of radar and gauge rainfall data," *Journal of Hydrometeorology*, vol. 13, no. 6, pp. 1939–1953, 2012.

[4] M. L. Baeck and J. A. Smith, "Rainfall estimation by the WSR-88D for heavy rainfall events," *Weather and Forecasting*, vol. 13, no. 2, pp. 416–436, 1998.

[5] GJ. Ciach, W. F. Krajewski, and V. Gabriele, "Product-error-driven uncertainty model for probabilistic quantitative

precipitation estimation with NEXRAD data," *Journal of Hydrometeorology*, vol. 8, no. 6, pp. 1325–1347, 2007.

[6] L. Delobbe, D. Dehem, P. Dierickx, E. Roulin, M. Thunus, and C. Tricot, "Combined use of radar and gauge observations for hydrological applications in the Walloon Region of Belgium," in *Proceedings of the Fourth European Conference on Radar in Meteorology and Hydrology (ERAD 2006)*, pp. 418–421, Barcelona, Spain, September 2006.

[7] D. P. Jorgensen and P. T. Willis, "A *Z-R* relationship for hurricanes," *Journal of Applied Meteorology*, vol. 21, no. 3, pp. 356–366, 1982.

[8] J. S. Marshall and W. M. Palmer, "The distribution of raindrops with size," *Journal of Meteorology*, vol. 5, no. 4, pp. 165-166, 1948.

[9] JS. Marshall, R. C. Langille, and W. M. Palmer, "Measurement of rainfall by radar," *Journal of Meteorology*, vol. 4, no. 6, pp. 186–192, 1947.

[10] D. Rosenfeld, D. B. Wolff, and D. Atlas, "General probability-matched relations between radar reflectivity and rain rate," *Journal of Applied Meteorology*, vol. 32, no. 1, pp. 50–72, 1993.

[11] B. E. Vieux and P. B. Bedient, "Estimation of rainfall for flood prediction from WSR-88D reflectivity: a case study, 17-18 October 1994," *Weather and Forecasting*, vol. 13, no. 2, pp. 407–415, 1998.

[12] R. A. Fulton, J. P. Breidenbach, D.-J. Seo, and D. A. Miller, "The WSR-88D rainfall algorithm," *Weather and Forecasting*, vol. 13, pp. 377–395, 1998.

[13] M. Filliers, T. Rijsselaere, P. Bossaert et al., "A microphysical interpretation of radar reflectivity–rain rate relationships," *Journal of the Atmospheric Sciences*, vol. 61, no. 61, pp. 1114–1131, 2004.

[14] D. Atlas, C. W. Ulbrich, F. D. Marks Jr., E. Amitai, and C. R. Williams, "Systematic variation of drop size and radar-rainfall relations," *Journal of Geophysical Research: Atmospheres*, vol. 104, no. D6, pp. 6155–6169, 1999.

[15] G. W. Lee and I. Zawadzki, "Variability of drop size distributions: time-scale dependence of the variability and its effects on rain estimation," *Journal of Applied Meteorology*, vol. 44, no. 2, pp. 241–255, 2005.

[16] O. P. Prat and A. P. Barros, "Exploring the transient behavior of *Z-R* relationships: implications for radar rainfall estimation," *Journal of Applied Meteorology and Climatology*, vol. 48, no. 10, pp. 2127–2143, 2009.

[17] C. W. Ulbrich and L. G. Lee, "Rainfall measurement error by WSR-88D radars due to variations in *Z-R* law parameters and radar constant," *Journal of Atmospheric and Oceanic Technology*, vol. 16, no. 8, pp. 1017–1024, 1999.

[18] D. Rosenfeld and C. W. Ulbrich, "Cloud microphysical properties, processes, and rainfall estimation opportunities," in *Radar and Atmospheric Science: A Collection of Essays in Honor of David Atlas, Meteorological Monographs*, pp. 237–258, American Meteor Society, Geneseo, NY, USA, 2003.

[19] S. Chumchean, A. Sharma, and A. Seed, "An integrated approach to error correction for real-time radar-rainfall estimation," *Journal of Atmospheric and Oceanic Technology*, vol. 23, no. 1, pp. 67–79, 2006.

[20] J. Liu, Z. Song, D. Liu, C. Jia, and S. Xu, "Classified *Z-I* relationship and its application to the measurement of rainfall by weather radar over the Huaihe River Basin," *Scientia Meteorologica Sinica*, vol. 19, pp. 213–220, 1999, in Chinese.

[21] L. Alfieri, P. Claps, and F. Laio, "Time-dependence *Z-R* relationships for estimating rainfall fields from radar measurements," *Natural Hazards and Earth System Sciences*, vol. 10, no. 1, pp. 149–158, 2010.

[22] Y. Wang, Y. Feng, J. Cai, and S. Hu, "An approach for radar quantitative precipitation estimate based on categorical *Z-I* relations," *Journal of Tropical Meteorology*, vol. 27, pp. 601–608, 2011, in Chinese.

[23] R. F. Adler and R. A. Mack, "Thunderstorm cloud height-rainfall rate relations for use with satellite rainfall estimation techniques," *Journal of Applied Meteorology*, vol. 23, no. 2, pp. 280–296, 1984.

[24] D. Atlas, D. Rosenfeld, and D. A. Short, "The estimation of convective rainfall by area integrals. 1. The theoretical and empirical basis," *Journal of Geophysical Research*, vol. 95, no. D3, pp. 2153–2160, 1990.

[25] D. Rosenfeld, D. Atlas, and D. A. Short, "The estimation of convective rainfall by area integrals: 2. the height-area rainfall threshold (HART) method," *Journal of Geophysical Research*, vol. 95, no. D3, pp. 2161–2176, 1990.

[26] K. M. Bedka, C. Wang, R. Rogers, L. D. Carey, W. Feltz, and J. Kanak, "Examining deep convective cloud evolution using total lightning, WSR-88D, and GOES-14 super rapid scan datasets," *Weather and Forecasting*, vol. 30, no. 3, pp. 571–590, 2015.

[27] J. Van Andel, "Radar echo classifier algorithm development using Python," in *Proceedings of International Conference on Radar Meteorology*, pp. 704–706, American Meteorological Society, Boston, MA, USA, July 2001.

[28] X. Gao, J. Liang, and C. Li, "Radar quantitative precipitation estimation techniques and effect evaluation," *Journal of Tropical Meteorology*, vol. 28, no. 1, pp. 77–88, 2012, in Chinese.

[29] G. Delrieu, B. Boudevillain, J. Nicol et al., "Bollène-2002 experiment: radar quantitative precipitation estimation in the Cévennes-Vivarais region, France," *Journal of Applied Meteorology and Climatology*, vol. 48, no. 7, pp. 1422–1447, 2009.

[30] H. Zou, S. Zhang, X. Liang et al., "Improvement in the methods for removing isolated non-meteorological echoes and ground clutter in CINRAD," *Journal of Meteorological Research*, vol. 32, no. 4, pp. 1–14, 2018.

[31] Y. Xiao, L. Liu, and S. Yan, "Study of methods for three-dimensional multiple-radar reflectivity mosaics," *Journal of Meteorological Research*, vol. 22, no. 3, pp. 351–361, 2008.

[32] V. Lakshmanan, K. Hondl, C. K. Potvin, and D. Preignitz, "An improved method for estimating radar echo-top height," *Weather and Forecasting*, vol. 28, no. 2, pp. 481–488, 2013.

[33] J. Zhang, K. Howard, and J. J. Gourley, "Constructing three-dimensional multiple-radar reflectivity mosaics: examples of convective storms and stratiform rain echoes," *Journal of Atmospheric and Oceanic Technology*, vol. 22, no. 1, pp. 30–42, 2005.

[34] P. Zhang, T. Dai, D. Wang, and B. Lin, "Derivation of the *Z-I* relationship by optimization and the accuracy in the quantitative rainfall measurement," *Scientia Meteorologica Sinica*, vol. 12, pp. 334–338, 1992, in Chinese.

[35] G. J. Ciach, W. F. Krajewski, E. N. Anagnostou et al., "Radar rainfall estimation for ground validation studies of the tropical rainfall measuring mission," *Journal of Applied Meteorology*, vol. 36, no. 6, pp. 735–747, 1997.

[36] G. Held, W. F. Krajewski, E. N. Anagnostou et al., "The probability of hail in relation to radar echo heights on the South African Highveld," *Journal of Applied Meteorology*, vol. 17, no. 6, pp. 755–762, 1978.

[37] A. I. Watson, R. L. Holle, and R. E. López, "Lightning from two national detection networks related to vertically integrated liquid and echo-top information from WSR-88D

radar," *Weather and Forecasting*, vol. 10, no. 3, pp. 592–605, 1995.

[38] Y. He, Y. Zhang, R. Kuligowski et al., "Incorporating satellite precipitation estimates into a radar-gauge multi-sensor precipitation estimation algorithm," *Remote Sensing*, vol. 10, no. 2, p. 106, 2018.